EIGEN-FREQUENCY CONTROL DESIGN OF CFRP STRUCTURES USING AN EMBROIDERY MACHINE

Tadashige Ikeda[+1], Kosuke Oka[+2] and Tatsuya Nishida[+3]

[+1-3]Department of Aerospace Engineering, Nagoya University, Nagoya, Japan

To raise the flutter speed of an airplane wing, increase in frequency margin between its fundamental torsional and bending modes is effective. Recently fiber reinforced plastic (FRP) laminates came to be widely used as the primary structures of airplanes, which can control the mechanical properties and the eigen-frequencies by the laminate stacking sequence, ply orientation, and so on. Moreover, if curved paths of the fibers can be allowed, the structure can be designed more lightly and accordingly the airplane can show higher performances. To this end a tailored fiber placement (TFP) method using an embroidery machine was suggested. In this paper, feasibility of the TFP with the embroidery machine was examined for the eigne-frequency control of a cantilever rectangular laminate plate as a preliminary study of applications of the TFP method to the flutter problems. First, the method to estimate material constants of a TFP layer and substrate layers was proposed according to the classical laminate theory. Then, using the obtained material constants an optimal fiber bundle path was calculated for the cantilever rectangular laminate plate with a size of 150mm×100mm×2mm so that the frequency margin between the fundamental torsional and bending modes was maximized keeping the fundamental frequency of the bending mode more than 80 Hz. Experimental verification was also performed. The prediction agreed well with the experiment, differing by approximately 10% due to the manufacturing error and the assumptions. Next to design further light structures a method that the stiffening fiber bundles were locally placed was proposed. The optimization result of the local TFP showed it had a comparable performance yet less than a half of weight of the reinforcing fiber bundles compared to the global TFP. These results indicate feasibility of application of the TFP to the aeroelastic problems.

Keyword: eigen-frequency, CFRP, tailored fiber placement, embroidery, flutter.

1. INTRODUCTION

Raising flutter speed is one of the challenges of aircraft design since the flutter leads to reduction of operational safety and durability of the aircraft structure. According to the classical theory of aeroelasticity, it is known that large frequency margin between the fundamental torsional and the fundamental bending modes is effective to raise the flutter speed of an airplane wing. With respect to the airplane structures, recently fiber reinforced plastics (FRPs) came to be used as the primary structures because of their high specific strength and corrosion resistance. However, the strength and stiffness of FRP plates significantly depend on the angle between the fiber and load direction. If the direction of the loads is different form the fiber by 5°, the strength reduces by more than 60% for instance. Because of such anisotropic properties, the mechanical properties of the laminates can be controlled by arranging the stacking sequence and ply orientation. The aeroelastic properties can be also improved by this arrangement. This technology is referred to as the aeroelastic tailoring and have been studied actively since 1970's, although the first patent was filed in 1949[1] according to Ref. 2. The state-of-art for aeroelastic tailoring and related research were well overviewed in Ref. 3 published recently.

In the traditional aeroelastic tailoring, the stacking sequence and ply orientation of prepregs with unidirectional fibers are arranged. If the fibers can be placed along a desired path, not only straight but also curved, the laminates can be designed more lightly and more optimally. To this end tailored fiber placement

---

(TFP) methods[4-10] can be suggested. However, the TFP methods have been still hardly applied to the aeroelastic problems[11]. With respect to the TFP itself, some researchers use prepreg tows for processing the laminates[4,5], while others use dry tows, in which the dry tows are placed on a substrate by using an embroidery machine and impregnated with resin[6-10]. The former method uses costly prepregs, freezers to store them, and autoclaves to harden them, while the latter method does not use such materials and facilities. Accordingly the composites processed by the latter method are expected to be lower-cost. Hence we have studied the embroidery-based TFP. Oka et al.[12] proposed a design method for the embroidery-based TFP and verified its availability for a static bending-torsion problem of a cantilever plate. Then, Nishida et al.[13] and Oka et al.[14] applied this method to a dynamic problem of controlling eigen-frequencies of the cantilever plate. In this paper, these results are introduced as a preliminary study for application of the embroidery-based TFP method to the aeroelastic problems.

2. EMBROIDERY-BASED TFP

In this study the embroidery-based TFP method was applied. The embroidery machine used here is shown in Fig. 1 (Tajima, TCWM-101). When a desired path of the carbon fiber bundle was input to the embroidery machine, the machine placed a continuous reinforcement fiber bundle on the desired path on a substrate and processed a dry preform. A pair of the preforms were symmetrically put together as shown in Fig. 3, and impregnated with resin by using the vacuum assisted resin transfer molding method (VaRTM). Here a carbon fiber bundle (Toho Tenax, HTA40-12K) was used as the reinforcement fiber, plain woven carbon fabrics (Toho Tenax, W3101) with a stacking sequence of $(45^{o}/0^{o})$ were used as the substrate, and epoxy resin (Nagase Chemtex, XNR/H6815) was used as the resin.

3. ESTIMATION OF ELASTIC MODULI OF EACH LAYER[13]

Stiffness of the TFP layer is affected by the embroidery effects of not only holes opened by a needle and the threads included but also interval between neighboring fiber bundle paths and thickness variation due to the variation of the interval. The interval, d, and the thickness, t, are related to the fiber bundle direction, θ, in the applied embroidery-based TFP.

$$d=d_0\cos\theta, \tag{1}$$

where d_0 is the interval between the neighboring fiber bundle paths along the reference direction defined as $\theta = 0^{o}$ here, as shown in Fig. 2.

To predict the mechanical properties and to design the laminate structures having TFP layers precisely, the embroidery effects must be involved in the stiffness matrix of each layer. The stiffness matrix and the thickness of the TFP layer must be given by functions of the fiber bundle angle, θ, or the interval, d, and accordingly they must vary during the optimization design process.

The stacking sequence of the TFP laminate plates considered here was $[\text{TFPL}/45^{o}/0^{o}]_S$. TFPL represents the TFP layer, a pair of square brackets represent the laminates stitched together by the threads, and the subscript S represents that a pair of the stitched preforms are symmetrically put together. Accordingly, the TFP laminate plates were comprised of a pair of TFP layers with the threads in the transversal direction and in-plane direction, a pair of plain woven layers in 45° direction with the threads in the transverse direction, and a pair of plain woven layers in 0° direction with the threads in the transverse direction and in-plane direction. These three kinds of layers are referred to as TFPL, PW_{mid}, and PW_{in}, respectively, as shown in Fig. 3.

To obtain the mechanical properties including the embroidery effects in each layer, $[\text{TFPL}0^{o}/45^{o}/0^{o}(d)]_S$, $[0^{o}/0^{o}(d)]$, $[0^{o}/0^{o}(d)]_S$, $[0^{o}/45^{o}/0^{o}(d)]_S$ were processed and the mechanical properties of the laminate plates were measured by tensile tests. $\text{TFPL}0^{o}$ represents the TFP layer with fiber bundles placed in the 0° direction on the substrate, d represents the interval between neighboring fiber bundle paths, and (d) represents that their mechanical properties are functions of the interval. Although the interval should be related to the fiber bundle angle, θ, with Eq. (1) in the practical TFP laminate plates, only the interval was varied keeping the fiber bundle angle at 0° here. This is because it was assumed that the angle between the direction

of the fiber bundles and the substrate did not affect the mechanical properties of the TFP layer and the substrate layers. The mechanical properties of each layer against the interval were calculated by using the classical laminate theory. In this study, the relationship between resultant forces and in-plane strains becomes

$$\begin{Bmatrix} N_x \\ N_y \\ N_{xy} \end{Bmatrix} = \begin{bmatrix} A_{11} & A_{12} & 0 \\ A_{12} & A_{22} & 0 \\ 0 & 0 & A_{66} \end{bmatrix} \begin{Bmatrix} \varepsilon_x \\ \varepsilon_y \\ \gamma_{xy} \end{Bmatrix}, \tag{2}$$

where

$$A_{ij} = \sum_{k=1}^{N} \left(Q_{ij} \right)_k t_k , \quad (Q_{11})_k = \frac{E_{x,k}}{1 - v_{xy,k} v_{yx,k}} , \quad (Q_{12})_k = \frac{v_{yx,k} E_{x,k}}{1 - v_{xy,k} v_{yx,k}} , \quad (Q_{22})_k = \frac{E_{y,k}}{1 - v_{xy,k} v_{yx,k}} ,$$

$$(Q_{66})_k = \frac{1}{\dfrac{4}{E_{45,k}} - \dfrac{1}{E_{x,k}} - \dfrac{1}{E_{y,k}} + \dfrac{2 v_{xy,k}}{E_{x,k}}} .$$

E and v denote Young's modulus and Poisson ratio, respectively, and the subscripts k, x, y, and 45 represent the material constants in k-th layer, and those in the x, y, and 45° direction, respectively. N, ε, and γ denote the resultant force, in-plane normal strain, and in-plane shearing strain.

The specimens [TFPL0°/45°/0°(d)]$_S$, [0°/0°(d)], [0°/0°(d)]$_S$, [0°/45°/0°(d)]$_S$ are referred to as TFP, PW$_2$, PW$_4$, and PW$_6$, respectively. Here it was assumed that the thickness and the material constants for the corresponding layer were consistent in PW$_2$, PW$_4$, PW$_6$, and TFP. More specifically, it was assumed that PW$_2$ consisted of (PW$_{sur}$)$_S$, PW$_4$ consisted of (PW$_{sur}$/PW$_{in}$)$_S$, PW$_6$ consisted of (PW$_{sur}$/PW$_{mid}$/PW$_{in}$)$_S$, and TFP consisted of (TFPL$_{0o}$/PW$_{mid}$/PW$_{in}$)$_S$. PW$_{sur}$ represents the plain woven layer in 0° direction with the threads in the transverse direction and in-plane direction on the surface, and it was distinguished from PW$_{in}$ because PW$_{sur}$ had irregular surface due to the peel ply and the distribution medium for VaRTM. The mechanical properties of PW$_{sur}$(d) can be obtained from those of PW$_2$(d), the mechanical properties of PW$_{in}$(d) can be obtained from those of PW$_4$(d) and PW$_{sur}$(d), the mechanical properties of PW$_{mid}$(d) can be obtained from those of PW$_6$(d), PW$_{sur}$(d), and PW$_{in}$(d), and the mechanical properties of TFPL$_{0o}$(d) can be obtained from those of TFP(d), PW$_{in}$(d), and PW$_{mid}$(d).

The tensile tests were carried out with a universal testing machine (Shimadzu, AG-5000B) following JIS K7164. The specimen size was 250mm×25mm. The 50mm regions of the both ends were clamped through sandpapers (#180) used as friction tabs. The displacement rate was 1.0mm/min. The strain was measured by strain gauges. The test was performed at room temperature of 23°C. The tensile moduli were calculated within the range between 500με and 2500με. The intervals, d, of the specimens were set to 2.0mm, 1.7mm, 1.4mm, 1.2mm, and 1.0mm, which corresponded to $\theta = 0^\circ$, 30°, 45°, 53°, and 60°, respectively, because d_0 was set to 2.0mm. Four specimens for each in the 0°, 45°, and 90° direction were cut out from the TFP plates, while four specimens for each in the 0° and 45° direction were cut out from the PW$_2$, PW$_4$, and PW$_6$ plates because the properties in the 90° direction was assumed to be the same as those in the 0° direction.

Fig. 4 shows the elastic moduli for each laminate plate. Closed symbols, error bars, and lines represent mean, standard deviation, and approximation line, respectively. The properties for PW$_2$, PW$_4$, and PW$_6$ can be assumed to be independent of the intervals, that is, amount of the holes and threads. The properties for TFP can be approximated by liner functions of the interval. The elastic modulus of TFP in the 0° direction decreases with increase in the interval, while the elastic moduli in the 45° and 90° direction increase with increase in the interval. The latter is attributed to the fact that the volume fraction of the TFP layer decreases and the volume fraction of the fibers in the 45° and 90° direction increases as the interval increases.

Substituting the obtained approximation values into the classical lamination theory, Eq. (2), the

material constants in the longitudinal and transversal direction of the fiber were estimated. They are listed in Table 1. The subscript L and T represent the longitudinal and transverse direction of the fiber, G and ρ denote the shearing modulus and the density, respectively. The material constants of TFPL were assumed to be a linear function again.

Open symbols in Fig. 4(d) represent the elastic moduli recalculated with the estimated material constants for each layer listed in Table 1. The recalculated moduli are seen to be in good agreement with the measured values and that indicates the validity of the assumption.

4. EIGEN-FEQUENCY CONTROL BY GLOBAL FIBER PLACEMENT[13]

(1) Formulation

To raise the flutter speed of an airplane wing, increase in frequency margin between its fundamental torsional and bending modes is effective. Hence here we considered a problem of finding an optimal fiber bundle path so that the frequency margin between the first and second modes of a [TFP/45°/0°]$_S$ laminate cantilever plate was maximized yet the first eigen-frequency was kept more than a certain frequency to maintain a certain level of bending stiffness. The size of cantilever plate was assumed to be 150mm by 100mm and the first eigen-frequency was kept more than 80Hz. This problem is specifically formulated as

$$
\begin{aligned}
&\text{Design variables:} && \boldsymbol{\theta} = [\theta_1, \cdots, \theta_{15}] \\
&\text{which minimalizes:} && f(\boldsymbol{\theta}) = -(Freq2 - Freq1); \\
&\text{subject to constrains:} && -60^{\circ} \le \theta_i \le 60^{\circ} \quad (i = 1, \cdots, 15), \\
& && |\theta_j - \theta_{j-1}| \le 15^{\circ} \quad (j = 2, \cdots, 15), \\
& && Freq1 \ge 80\text{Hz}.
\end{aligned}
\tag{3}
$$

The cantilever plate was divided by 15 elements along the longitudinal direction as shown in Fig. 5. θ_i, Freq1, and Freq2 denote the fiber bundle angle in the i-th element, the first, and the second eigen-frequency of the plate, respectively. The fiber bundle angle θ_i was limited within ±60° and the difference in fiber bundle angle between the neighboring elements was limited within ±15°. The subproblem approximation method built in ANSYS ver. 12 and a kind of sweeping methods were applied to optimize the fiber bundle path of the TFP layer.

(2) Results and discussions

The optimal path for this problem is shown in Fig. 6 and the first and the second eigen-frequency in this case are listed in Table 2. The eigen-frequencies of the plates having TFP layers with a uniform fiber bundle angle of 0°, 45°, and 60° were also calculated. Of course, the eigen-frequencies were not controlled in these cases.

The first vibration mode was bending and the second vibration mode was twisting. It is seen from Fig. 6 that the fiber bundle angle became close to 0° around the root and 50° around the middle of the plate. The former may affect increasing the first eigen-frequency and the latter may affect increasing the second eigen-frequency. It is seen that the constraint of the first eigen-frequency equal or more than 80 Hz is not satisfied for the plates with uniform fiber directions of 45° and 60°, and that the plate with the optimal placement of fibers is surely optimized for the objective function under the constraints. The validity of the predicted results was verified by comparing to experimental results. A specimen was clamped by a vice. Vibration was generated by giving an impact with a hammer. The vibration was measured by a strain gauge. The obtained eigen-frequencies are also listed in Table 2.

The measured eigen-frequencies agree well with calculated ones, which have a margin of error of approximately 10% due to manufacturing errors of the plates for the example problem and for measurement of the material constants, the assumption for estimation of the material constants, and so on. Considering the errors, the calculated optimal fiber path is approximately optimal in the experiment, although the constraint of the first eigen-frequency is not satisfied. The first eigen-frequency cannot be known before the experiment.

Such a value might not be adequate to be included in the constraints because experiments involve errors. Nevertheless, when a structural optimization must be carried out with such constraints, the error margin should be considered.

5. EIGEN-FEQUENCY CONTROL BY LOCAL FIBER PLACEMENT[14]
(1) Formulation

In the previous section the reinforcing fiber bundles were placed over the whole substrate. However, if the fiber bundles could be placed locally, the weight could be reduced and the performance could be improved more. Therefore here the local fiber placement is considered for the same objective in the previous section that is the frequency margin between the first and second modes was maximized yet the first eigen-frequency was kept more than 80Hz. This problem is specifically formulated as

$$
\begin{aligned}
&\text{Design variables:} && \mathbf{t} = [t_1, \cdots, t_N] \\
&\text{which minimalizes:} && f(\mathbf{t}) = -(Freq2 - Freq1); \\
&\text{subject to constrains:} && Freq1 \geq 80\text{Hz}, \\
& && m_f \leq m_{f\max}.
\end{aligned}
\tag{4}
$$

Here, i is the element ID, t_i is the thickness of the i-th element, N is the number of the elements, m_f is the mass fraction of a TFPL to the TFPL filled with fiber bundles in the 0°-direction, and $m_{f\max}$ is the maximum value of m_f, which were assumed to be 0.3, 0.4, and 0.5 here. In this optimization problem, the fiber bundle angle in TFPL was fixed at 0° and the thickness distribution was optimized for the objective.

(2) Results and discussions

The first eigen-frequency and the frequency margin between the first and the second eigen-frequencies are listed in Table 3 for the three $m_{f\max}$. For reference those of the global TFP are also listed for the optimal fiber bundle path and 0° fiber bundle path. Figure 7 shows an optimal thickness distribution and assumed fiber paths for the local TFP that was optimized under the constraint $m_{f\max} = 0.4$. From Table 3, the largest margin between the first and the second eigen-frequency is the one for the global TFP with the optimal fiber bundle path. The mass fraction of this case is 1.0 or more value, because the density of TFPL depends on a fiber bundle angle and $m_f = 1.0$ was defined for the TFPL filled with fiber bundles in the 0°-direction. On the other hand, the result for the local TFP shows comparable performance yet with less than a half of the mass fraction of the global TFP. From the three results of the local TFP, the margin between the two eigen-frequencies reduces as the mass fraction decreases. The constraint about the mass fraction should be determined from the trade-off between the performance and the weight. There are three thick regions in TFPL as shown in Fig. 7. Two are located near the fixed edge and one is located from the center to the tip. It is considered that two thick regions near the fixed edge are effective to increase the first and the second eigen-frequencies by increasing the stiffness for the both the bending and twisting modes, and that another thick region from the center to the tip is effective to decrease the first eigen-frequency without decreasing the second eigen-frequency by increasing the inertia for the bending mode.

5. CONCLUSIONS

A TFP method using an embroidery machine was suggested to raise the flutter speed of an airplane wing by controlling eigen-frequencies of the structure. This method was verified by a preliminary example problem of controlling eigen-frequencies of a cantilever plate. First, the method to estimate material constants of a TFP layer and substrate layers was proposed according to the classical laminate theory. Then, using the obtained material constants an optimal fiber bundle path was calculated for the cantilever plate so that the frequency margin between the fundamental torsional and bending modes was maximized with a constrain of the fundamental frequency of the bending mode kept more than a certain frequency value. A desired result could be obtained by an optimization calculation. The carbon fiber bundles were placed along the desired path

on plain woven carbon fabrics by an embroidery machine and the preform was impregnated by using VaRTM method. The eigen-frequencies of the laminate plate agreed well with the calculated results with an error of approximately 10%. Accordingly, it was found that the error margin should be considered when an optimization result is realized. Next a local TFP method was proposed to reduce the weight more. The optimization result of the local TFP showed it had a comparable performance yet less than a half of weight of the reinforcing fiber bundles compared to the global TFP. This result indicates that the local TFP is more effective to design high performance yet light laminates.

In this paper a passive eigen-frequency control with the TFP was introduced as a preliminary study for the aeroelastic problems by placing passive carbon fiber bundles on a substrate optimally. Furthermore a method to place shape memory alloy wires on a TFP layer has been also proposed in our laboratory[15]. Combining such an active material with the passive materials must expand the limitations of not only aeroelastic problems but also aerodynamic and structural problems.

ACKNOWLEDGMENT

REFERENCES

1) Munk, M.: Propeller containing diagonally disposed fibrous material, *U.S. Patent* 2,484,308,1111, 1949.
2) Shirk, M., Hertz, T., and Weisshaar, T.: Aeroelastic tailoring – theory, practice, promise, *J. Aircraft*, Vol. 23, No. 1, pp. 6-18, 1986.
3) Jutte, C. V. and Stanford, B. K.: Aeroelastic tailoring of transport aircraft wings: State-of-the-art and potential, *NASA/TM*-2014-218252, pp. 1-29, 2014.
4) Tatting, B. F. and Gürdal, Z.: Design and manufacture of elastically tailored tow placed plates, *NASA/CR*, 211919, 2002.
5) Gürdal, Z. and Tatting, B. F.: Tow-placement technology and fabrication issues for laminated composite structures, *Proc. 46th AIAA/ASME/ASCE/AHS/ASC SDM Conf.*, Austin, U.S.A., AIAA 2005-2017, pp. 1-18, 2005.
6) Crothers, P. J., Drechsler, K., Feltin, D., Herszberg, I., and Kruckenberg, T.: Tailored fiber placement to minimise stress concentrations, *Composites Part A*, Vol. 28A, pp. 619-625, 1997.
7) Mattheij, P., Gliesche, K., and Feltin, D.: 3D reinforced stitched carbon/epoxy laminates made by tailored fibre placement, *Composites Part A*, Vol. 31, pp. 571-581, 2000.
8) Temmen, H., Degenhardt, R., and Raible, T.: Tailored fibre placement optimization tool, *Proc. 25th ICAS*, Hamburg, Germany, ICAS2006-4.8.3, pp. 1-10, 2006.
9) Hazra, K., Saverymuthapulle, M., Hawthorne, M., Stewart, D. L., Weaver, P., and Potter, K.: Investigation of mechanical properties of tow steered CFRP panels, *Proc. ICCM17*, Edinburgh, Scotland, D11-5, pp. 1-11, 2009.
10) Panesar, A. S., Hazra, K., and Weaver, P. M.: Investigation of thermally induced bistable behaviour for tow-steered laminates, *Composites Part A*, Vol. 43, pp. 926-934, 2012.
11) Haddadpour, H. and Zamani, Z.: Curvilinear fiber optimization tools for aeroelastic design of composite wings, *J. Fluids Struct.*, Vol. 33, pp. 180-190, 2012.
12) Oka, K., Ikeda, T., Senba, A., and Ueda, T.: Design of CFRP with fibers placed by using an embroidery machine, *Proc. ICCM18*, Jeju Island, Korea, M32-2, pp. 1-5, 2011.
13) Nishida, T., Ikeda, T., and Senba, A.: Optimal fiber placement including effects of embroidery, *Proc. ICCM19*, Montreal, Canada, pp. 3865-3872, 2013.
14) Oka, K., Ikeda, T., and Senba, A. : Optimal placement design of fibers partially set by an embroidery machine, *Proc. APISAT-2013*, Takamatsu, 07-03-3, pp. 1-4, 2013.
15) Torii, N., Oka, K., and Ikeda, T.: Creation of smart composites using an embroidery machine, *Proc. SPIE*, Vol. 9800, Las Vegas, U.S.A, 2016.
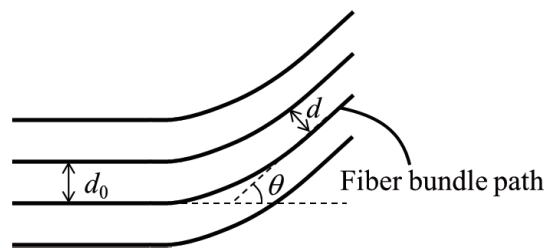
Figure 1: Embroidery machine. Tajima TCWM-101.

Figure 2: Variation of interval between the neighboring fiber bundle paths due to the fiber bundle angle.
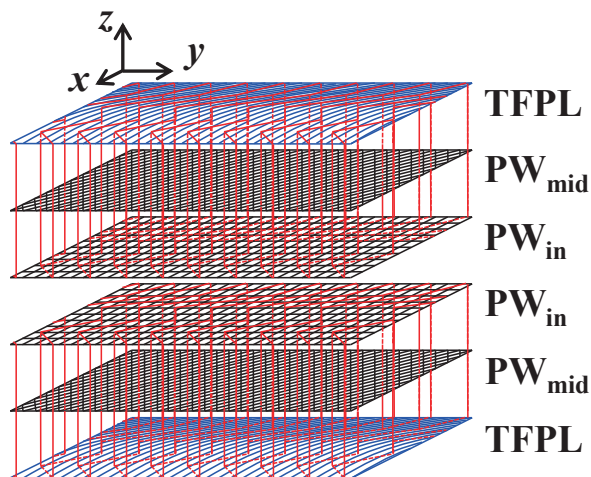

Figure 3: Schematic diagram of the laminate with stacking sequence [TFPL/45°/0°]$_S$. Red lines represent the stitched threads.

(a) PW_2 (b) PW_4
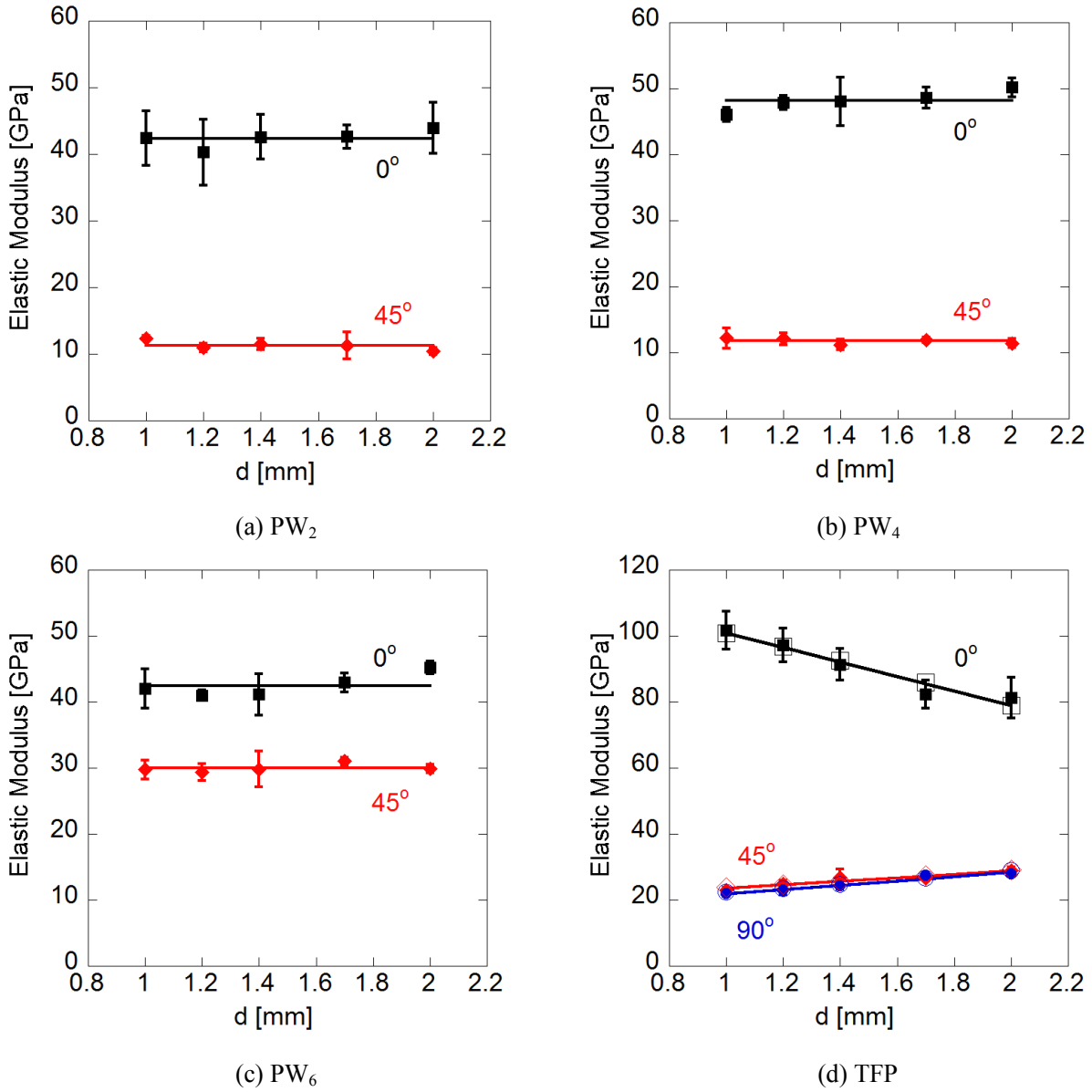
(c) PW_6 (d) TFP

Figure 4: Elastic moduli of the various laminate plates[13].
Closed symbols, error bars, and lines represent mean, standard deviation, and approximation line, respectively.
Open symbols in (d) represent the elastic moduli recalculated by using the estimated material constants for
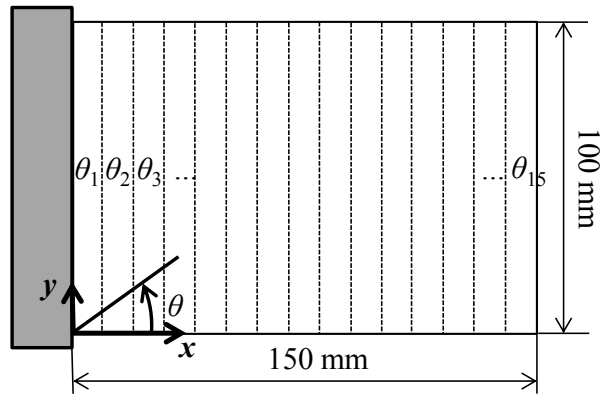each layer listed in Table 1.
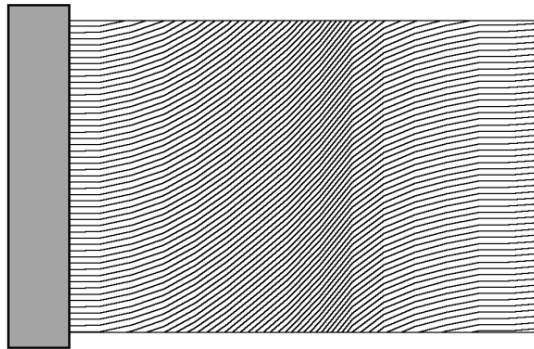
Figure 5: Cantilever plate of the example problem.
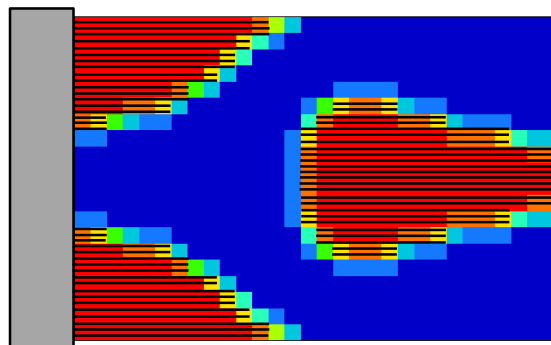

Figure 6: Optimal fiber bundle path[13].

Figure 7: Thickness distribution and assumed fiber path of the local TFP ($m_{f\mathrm{max}} = 0.4$)[14].

Table 1: Estimated material constants for each layer[13].

	PW$_{in}$	PW$_{mid}$	TFPL(d [mm])
E_L [GPa]	54.5	59.7	-14.2d+154.5
E_T [GPa]	-	-	1.9d+4.7
v_{LT}	0.08	0.12	0.02d+0.34
v_{TL}	-	-	0.008d+0.009
G_{LT} [GPa]	3.6	5.2	0.4d+3.8
t [mm]	0.26	0.23	-0.3d+1.1
ρ [g/cm^3]	1.4	1.3	-0.09d+1.69

Table 2: Calculated and measured first eigen-frequency and margin between the first and the second eigen-frequencies in Hz for various fiber bundle paths[13].

Fiber bundle angle		0º	45º	60º	Optimal
Calculation	Freq1	110	58	49	80
	Freq2-Freq1	94	194	177	180
Experiment	Freq1	101	52	54	72
	Freq2-Freq1	83	172	182	158

Table 3: Optimization results of the global TFP and the local TFP[14].

	Global TFP	Local TFP		
		$m_{fmax} = 0.30$	$m_{fmax} = 0.40$	$m_{fmax} = 0.50$
Fiber bundle angle	Optimal	0º		
m_f	$\geqq 1.0$*	1.0	0.30	0.40	0.45
Freq1	80	110	80	80	80
Freq2-Freq1	180	94	148	154	154